

# Vapor pressures in the {Al(l) + Al<sub>2</sub>O<sub>3</sub>(s)} system: Reconsidering Al<sub>2</sub>O<sub>3</sub>(s) condensation

Evan Copland \*

Case Western Reserve University, NASA Glenn Research Center, Department of Materials Science and Engineering,  
21000 Brookpark Rd. MS 106-1, Cleveland, OH 4135, USA

Received 15 April 2005; received in revised form 17 June 2005; accepted 17 June 2005  
Available online 10 August 2005

## Abstract

The vaporization behavior of the Al–O system has been studied on numerous occasions but significant uncertainties remain. The origin of this uncertainty must be understood before Al–O vaporization behavior can be accurately determined. The condensation of Al<sub>2</sub>O<sub>3</sub> and clogging of the effusion orifice is a difficult problem for the Knudsen effusion technique that influences the measured vaporization behavior but has only received limited attention. This study reconsiders this behavior in detail. A new theory for Al<sub>2</sub>O<sub>3</sub> condensation is proposed together with procedures that will improve the measured thermodynamic properties of Al–O vaporization.

© 2005 Elsevier Ltd. All rights reserved.

**Keywords:** Al(g) and Al<sub>2</sub>O(g) vaporization; Al<sub>2</sub>O<sub>3</sub>(s) condensation; Improving thermodynamic measurements; Multiple effusion cell mass spectrometry

## 1. Introduction

The vaporization behavior of the Al–O system has been investigated in numerous studies since the early 1950s. These studies used the effusion method, in its various forms, to sample the vapor phase in equilibrium with {Al(l) + Al<sub>2</sub>O<sub>3</sub>(s)} [1–4] and Al<sub>2</sub>O<sub>3</sub>(s) [1,5,6] in a range of container materials. In spite of this level of investigation, some vapor species and the thermodynamics of vaporization are still not fully understood. Recently, there has been renewed interest in Al–O vaporization [7–9]. Improving the thermodynamic data of the Al–O system will allow more accurate measurements of the {alloy + oxide} equilibrium in the Ni–Al, Ti–Al and Fe–Al systems [10]. This information will improve our understanding of high-temperature oxidation behavior of these systems which rely on the formation of

a protective Al<sub>2</sub>O<sub>3</sub>(s) surface-layer by reaction with oxygen-containing atmospheres.

A range of vapor species have been identified in the Al–O system: Al(g), Al<sub>2</sub>O(g), Al<sub>2</sub>(g), AlO(g), AlO<sub>2</sub>(g), Al<sub>2</sub>O<sub>2</sub>(g), Al<sub>2</sub>O<sub>3</sub>(g), O(g), and O<sub>2</sub>(g) [1–6]. Questions remain about the existence of AlO<sub>2</sub>(g) [8]. The composition of the vapor depends on the oxygen partial pressure. At low  $p(\text{O}_2)$ , when Al(s,l) and  $\alpha\text{-Al}_2\text{O}_3(\text{s,l})$  are stable, Al(g) and Al<sub>2</sub>O(g) dominate while at higher  $p(\text{O}_2)$ , when  $\alpha\text{-Al}_2\text{O}_3(\text{s,l})$  is stable, O(g), Al(g), and AlO(g) typically dominate. To quantify the uncertainty in Al–O vaporization, reaction enthalpies measured by this author are compared to the accepted values [11–13] in table 1. The details of these new measurements will be discussed in a subsequent paper. While these results differ significantly, it is not constructive to propose changing generally accepted thermodynamic properties without first investigating possible reasons for the discrepancies and suggesting improved experimental procedures. Accordingly, two likely sources of error are: (1)

\* Tel.: +1 216 433 3738.

E-mail address: [evan.h.copland@grc.nasa.gov](mailto:evan.h.copland@grc.nasa.gov).

TABLE 1  
Comparison of reaction enthalpies in {Al(l) + Al<sub>2</sub>O<sub>3</sub>(s)} system, Δ<sub>R</sub>H<sup>o</sup>(298.15 K)

Reaction	Measured [14] (kJ · mol <sup>-1</sup> )	IVTAN [11] (kJ · mol <sup>-1</sup> )	JANAF [12] (kJ · mol <sup>-1</sup> )
Al(s,l) = Al(g)	341.0 ± 2.2	330.0 ± 3.0	329.7 ± 4.2
4/3Al(s,l) + 1/3Al <sub>2</sub> O <sub>3</sub> (s) = Al <sub>2</sub> O(g)	414.2 ± 3.6	409.0 ± 56	413.4 ± 50
4/3Al(g) + 1/3Al <sub>2</sub> O <sub>3</sub> (s) = Al <sub>2</sub> O(g)	-41.1 ± 3.2	-30.0 ± 4.3	-26.2 ± 3.0
2Al(g) + O(g) = Al <sub>2</sub> O(g)	-1075.5 ± 9.0	-1057.0 ± 20	-1053.7 ± 150

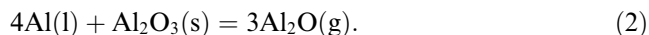
reaction between Al(l) and the effusion-cell material and (2) clogging the effusion orifice at high temperatures with the condensation of Al<sub>2</sub>O<sub>3</sub>(s).

Identifying a suitable container material is important for all thermodynamic measurements and a range of materials (*i.e.*, BeO, TaC, ZrO<sub>2</sub>, Al<sub>2</sub>O<sub>3</sub>, Mo, and W) have been used in Al–O vaporization studies. Brewer and Searcy [1] used BeO and TaC effusion-cells but Al(l) reacted with both materials. Porter *et al.* [2], used a ZrO<sub>2</sub>-liner in a Ta effusion-cell without reporting any significant reaction. Motzfeldt *et al.* [3,4] successfully used a Al<sub>2</sub>O<sub>3</sub> effusion-cell. Mo and W have been used extensively to study the vaporization of Al<sub>2</sub>O<sub>3</sub> but both are unsuitable for Al(l). According to the condensed phase diagrams, Al–O [15], Al–Zr–O [16], and Al<sub>2</sub>O<sub>3</sub>–ZrO<sub>2</sub>–Y<sub>2</sub>O<sub>3</sub> [17,18], Al<sub>2</sub>O<sub>3</sub> is best suited for studying the vaporization of {Al(l) + Al<sub>2</sub>O<sub>3</sub>(s)} as ZrO<sub>2</sub>-based containers will react with Al(l). The effect of a ZrO<sub>2</sub>-based effusion-cell was recently considered by directly comparing the vapor pressures of Al(g) and Al<sub>2</sub>O(g) in equilibrium with Al(l) in a ZrO<sub>2</sub> effusion-cell and Al(l) in a Al<sub>2</sub>O<sub>3</sub> effusion-cell [7]. These results showed Al(l) remained pure and a Al<sub>2</sub>O<sub>3</sub>-layer formed on the inner surface of the ZrO<sub>2</sub> effusion-cell, effectively transforming it into an Al<sub>2</sub>O<sub>3</sub> effusion-cell and making it thermodynamically identical to Al(l)+Al<sub>2</sub>O<sub>3</sub>(s). While interesting, this result showed that a ZrO<sub>2</sub> effusion-cell does not change the measured vaporization behavior in the Al–O system. This leaves the difficult problem of Al<sub>2</sub>O<sub>3</sub> condensation.

Al<sub>2</sub>O<sub>3</sub> condensation has been observed by this author while measuring the vaporization behavior of {Al(l) + Al<sub>2</sub>O<sub>3</sub>(s)}, {β-NiAl + Al<sub>2</sub>O<sub>3</sub>(s)} and {γ-TiAl(s) + Y<sub>2</sub>O<sub>3</sub>(s)} and was previously observed for {Al(l) + Al<sub>2</sub>O<sub>3</sub>(s)} by Motzfeldt *et al.* [3,4] and for Al<sub>2</sub>O<sub>3</sub>(l) by Drowart *et al.* [5]. It occurs on the outer edge of the orifice, is more pronounced for small diameter orifices (less than about 1.0 mm) and is usually only noticed at temperatures above about *T* = 1500 K. Condensation of Al<sub>2</sub>O<sub>3</sub> will influence the measured vaporization behavior by changing the shape of the effusion orifice and therefore the rate of effusion independent of the partial pressures inside the effusion-cell. This behavior appears to be typical for systems with high aluminum activity, and it is surprising that it has only received limited discussion. Motzfeldt *et al.* appears to be the only research to consider this problem and their experiments and discussion are reviewed.

### 1.1. Motzfeldt's investigation of Al<sub>2</sub>O<sub>3</sub>-condensation

This problem was considered on two occasions while studying the vaporization of {Al(l) + Al<sub>2</sub>O<sub>3</sub>(s)} in an Al<sub>2</sub>O<sub>3</sub>(s) effusion-cell by a classical effusion method with continuous thermogravimetric monitoring of the rate of mass loss. The first study was conducted at *T* = 1585 and *T* = 1623 K in a tube furnace with a graphite heating element and with effusion orifices ranging from (0.8 to 8.0) mm in diameter [3]. The second study was at *T* = 1556 K in a furnace with a molybdenum heating element and with effusion orifices ranging from (0.6 to 2.9) mm in diameter [4]. In all experiments, pure Al(s) with excess Al<sub>2</sub>O<sub>3</sub>(s) was loaded into Al<sub>2</sub>O<sub>3</sub> effusion-cells. From previous mass spectrometric studies [2,5,6] Al(g) and Al<sub>2</sub>O(g) were assumed to be the dominant vapor species and it was explicitly assumed that there was no mass loss due to vaporization of the outer surface of the Al<sub>2</sub>O<sub>3</sub> effusion-cell and implicitly assumed that the effusion cell did not gain mass by reaction with the furnace environment. Following these assumptions the measured mass loss for the system (sample + effusion cell) was due solely to the effusion of Al(g) and Al<sub>2</sub>O(g) at partial pressures *p*(Al) and *p*(Al<sub>2</sub>O), according to the vaporization reactions equations (1) and (2).



This occurs at a rate (mol · s<sup>-1</sup>) for each species according to the Hertz–Knudsen relation equation (3)

$$dn_i/dt = p(i)A_oW_o(2\pi RM_iT)^{1/2}, \quad (3)$$

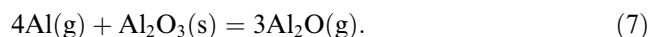
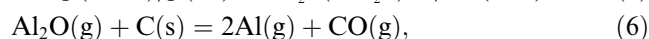
where *n<sub>i</sub>* is number of moles, *p*(*i*) is the partial pressure, *A<sub>o</sub>* is the area of the orifice, *W<sub>o</sub>* is the Clausing factor or the orifice, *R* is the gas constant, *M<sub>i</sub>* is the molar mass and *T* is the absolute temperature. The total mass loss, Δ*q*, is due to consumption of Al(l) and Al<sub>2</sub>O<sub>3</sub>(s) in the cell (Δ*q* = Δ*n*<sub>Al</sub> · *M*<sub>Al</sub> + Δ*n*<sub>Al<sub>2</sub>O<sub>3</sub></sub> · *M*<sub>Al<sub>2</sub>O<sub>3</sub></sub>). The moles of Al(l) consumed, Δ*n*<sub>Al</sub>, were determined by measuring how much Al(s) remained while Al<sub>2</sub>O<sub>3</sub>(s) consumption, Δ*n*<sub>Al<sub>2</sub>O<sub>3</sub></sub>, was determined by the difference between the total mass loss and measured Al(l) consumption (Δ*q* – Δ*n*<sub>Al</sub> · *M*<sub>Al</sub>)/*M*<sub>Al<sub>2</sub>O<sub>3</sub></sub>. For each mole of Al<sub>2</sub>O<sub>3</sub> four moles of Al(l) were consumed due to the effusion of three moles of Al<sub>2</sub>O(g) according to equation (2). The excess moles of Al(l) lost were attributed to reaction (1) and the effusion of Al(g). In this way the number of moles Al(g), *n*<sub>Al</sub>, and Al<sub>2</sub>O(g), *n*<sub>Al<sub>2</sub>O</sub>, lost by effusion

during the experiment were determined and used to calculate  $p(\text{Al})$  and  $p(\text{Al}_2\text{O})$  according to equation (3). The total rate of mass loss ( $\text{g} \cdot \text{s}^{-1}$ ) is the sum of the effusion of  $\text{Al}(\text{g})$  and  $\text{Al}_2\text{O}(\text{g})$ , equation (4), and is constant at a fixed temperature

$$dq/dt = A_o W_o / (2\pi RT)^{1/2} \times (p(\text{Al})(M_{\text{Al}})^{1/2} + p(\text{Al}_2\text{O})(M_{\text{Al}_2\text{O}})^{1/2}). \quad (4)$$

In both studies, however, the rate of mass loss was not constant but decreased with time. This was more pronounced for smaller effusion orifices and occurred at a faster rate in the first study. This behavior was attributed to  $\text{Al}_2\text{O}_3$  condensation on the outer edge of the orifice that reduced the orifice area,  $A_o$ , and changed the Clausing factor,  $W_o$ , during the course of each experiment. A temperature gradient was ruled out because no condensation was observed inside of the cell lid and a significant effort was made to ensure an isothermal condition. No explanation was proposed for  $\text{Al}_2\text{O}_3$  condensation in the first study but it was noted that the ratio of the measured partial pressures of the species,  $F$ , equation (5) was related to the effusion orifice area. It was suggested that this could be due  $\text{Al}_2\text{O}(\text{g})$  reacting with the graphite heating element and the formation of excess  $\text{Al}(\text{g})$  outside the effusion-cell, according to reaction (6). The excess  $\text{Al}(\text{g})$  could then react with the outside of the effusion-cell resulting in an increased loss of  $\text{Al}_2\text{O}_3(\text{s})$ , according to reaction (7). To test this a molybdenum heating element was used in the second study.

$$F = p(\text{Al}_2\text{O})/p(\text{Al}) = n_{\text{Al}_2\text{O}}(M_{\text{Al}_2\text{O}})^{1/2}/n_{\text{Al}}(M_{\text{Al}})^{1/2}, \quad (5)$$



The second study [4] used the same analysis procedure and similar behavior was observed but the rate of orifice clogging and the increase in  $F$  with orifice area was less pronounced. The variation in  $F$  with orifice area was accepted as real but unrelated to the heating element material. A complex calculation procedure was developed to consider an average effective orifice area,  $A_{\text{ave}}$ , to correct for the decreasing orifice area with time. In addition, the concept of “hindered” vaporization for  $\text{Al}(\text{g})$ ,  $\alpha_{\text{vap}}(\text{Al}) < 1$ , from  $\text{Al}_2\text{O}_3(\text{s})$  was introduced to explain the apparent decrease in measured  $p(\text{Al})$  with increasing orifice area (while  $p(\text{Al}_2\text{O})$  was assumed to be independent of orifice area). This was used, with reaction (7), to explain the “unavoidable”  $\text{Al}_2\text{O}_3$  condensation. The reduced  $p(\text{Al})$  in the effusion orifice acts to shift the equilibrium in reaction (7) to the left, resulting in condensation of  $\text{Al}_2\text{O}_3(\text{s})$ .

These studies clearly involved a large amount of detailed experimental work, however, there are several obvious problems in the interpretation of these results

that need to be identified. The first problem is the mass balance analysis used to determine the number of moles of  $\text{Al}(\text{l})$  and  $\text{Al}_2\text{O}_3(\text{s})$  lost from the system. The analysis technique did not allow the vaporization processes inside the cell and effusion from the cell to be treated separately from the condensation of  $\text{Al}_2\text{O}_3$  on the outside of the cell. A portion of material transported from inside the effusion-cell did not leave the system but condensed as  $\text{Al}_2\text{O}_3$  on the outside of the cell. Therefore, the measured mass loss is less than the actual amount of  $\text{Al}(\text{l})$  and  $\text{Al}_2\text{O}_3(\text{s})$  removed from inside of the cell. In this situation the analysis procedure underestimates the moles of  $\text{Al}_2\text{O}_3(\text{s})$  consumption which results in both a low  $p(\text{Al}_2\text{O})$  and high  $p(\text{Al})$ . As the amount of  $\text{Al}_2\text{O}_3$  condensation increases relative to the orifice area (as the orifice area decreases)  $F$  must decrease. Thus, the behavior observed for  $F$  can be explained without considering “hindered” vaporization of  $\text{Al}(\text{g})$  and the best results should be obtained with the largest orifices where the relative amount of orifice clogging is the smallest. While a reduced vaporization coefficient for  $\text{Al}(\text{g})$  from  $\text{Al}_2\text{O}_3(\text{s})$  is possible, its effect would be difficult to observe with a  $\{\text{Al}(\text{l}) + \text{Al}_2\text{O}_3(\text{s})\}$  mixture as  $\text{Al}(\text{g})$  vaporization from  $\text{Al}(\text{l})$  would dominate. As a general rule the more complex vapor species is more likely to experience hindered vaporization, that is  $\alpha_{\text{vap}}(\text{Al}_2\text{O}) < \alpha_{\text{vap}}(\text{Al})$  [19]. Further, if a reduced  $\alpha_{\text{vap}}(\text{Al})$  was the reason for  $\text{Al}_2\text{O}_3$  condensation then as the effusion orifice clogs  $p(\text{Al})$  would increase as it is more accurately sampled. This would shift equilibrium of reaction (7) to the right and limit further condensation, against the observation that  $\text{Al}_2\text{O}_3$  condensation is more pronounced for smaller orifices. These problems raise uncertainty about Motzfeldt’s theory. An obvious test of this theory is to measure  $F$  with time as the effusion orifice clogs due to  $\text{Al}_2\text{O}_3$  condensation. This is a relatively simple experiment for effusion cell vapor source coupled to a mass spectrometer, *KEMS*. This experiment is described and the results considered.

## 2. Experimental

### 2.1. Materials

In this study about 0.5 g of  $\text{Al}(\text{s})$  (99.9999 wt% purity) were loaded into an  $\text{Al}_2\text{O}_3$  effusion cell (99.99 wt% purity) shown schematically in figure 1. Prior to use, this effusion cell was cleaned by baking at about  $T = 1800 \text{ K}$  for 10 h under vacuum ( $\sim 10^{-3} \text{ Pa}$ ). In addition, a sample of  $\text{Au}$  (99.9999 wt% purity) was placed in a graphite-liner inside a second  $\text{Al}_2\text{O}_3$  effusion-cell, in the isothermal zone of the furnace, and was used to check for temperature and instrument sensitivity during the experiment.

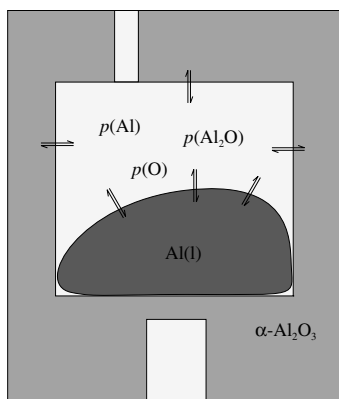


FIGURE 1.  $\text{Al}_2\text{O}_3$  effusion-cells: internal cell-body dimensions 10 mm diameter by 8.6 mm tall, orifice dimensions 1.0 mm diameter by 3.5 mm long. The orifice is offset by 2 mm from cell centerline while the hole in the bottom is part of blackbody source (2.5 mm in diameter by 13.5 mm long) used for temperature measurement.

## 2.2. Apparatus and experimental procedure

These measurements were made with a Nuclide/MAAS/PATCO 12-90-HT single focus magnetic sector mass spectrometer coupled to a multiple effusion-cell vapor source. The relative partial pressures of  $\text{Au}(\text{g})$ ,  $\text{Al}(\text{g})$ , and  $\text{Al}_2\text{O}(\text{g})$  were determined indirectly by sampling their flux in a molecular beam (selected from the distribution of effusing molecules) by electron impact resulting in  $\text{Au}^+$ ,  $\text{Al}^+$ , and  $\text{Al}_2\text{O}^+$  ions and the formation of a representative ion beam that was sorted according to mass-to-charge ratio by common mass spectrometric techniques. An electron energy of about 25 eV was used and there was no evidence of  $\text{Al}_2\text{O}(\text{g})$  fragmentation. The partial pressures,  $p(i)$ , in the effusion-cell is related to the measured intensity of each ion,  $I_i$ , and absolute temperature,  $T$ , by the following equation [20]:

$$p(i) = I_i T / S_i, \quad (8)$$

where  $S_i$  is the instrument sensitivity factor and is a complex function of the: intersection of the molecular and electron beams, ion extraction efficiency, ionization cross-section, transmission probability of the mass analyzer, detector efficiency and isotopic abundance. Absolute pressure measurements are difficult, as a result  $S_i$  is typically assumed constant and relative partial pressures are considered (*i.e.*,  $p(i) \propto I_i T$ ). In this way  $F$  was monitored directly by measuring the ion intensity ratio of  $\text{Al}_2\text{O}^+$  and  $\text{Al}^+$  with time, equation (9)

$$F \propto I_{\text{Al}_2\text{O}} / I_{\text{Al}}. \quad (9)$$

The effusion cells were maintained at  $T = 1550 \pm 3.0$  K over 8 h during which time a consistent portion of the effusing molecules from each cell were samples at 45 min

intervals while the orifice of the cell containing  $\text{Al}(\text{l})$  partial clogged with the condensation of  $\text{Al}_2\text{O}_3$ . From equation (3), the rate and the distribution of  $\text{Al}(\text{g})$  and  $\text{Al}_2\text{O}(\text{g})$  effusing from the orifice will change with time as the orifice closes. This will change their flux distribution in the molecular beam and therefore the rate of ion production independent of  $p(\text{Al}_2\text{O})$  and  $p(\text{Al})$  in the effusion-cell, however, as both species are sampled with the same orifice the effect is identical.

The successful application of a multiple effusion-cell vapor sources requires that vapor pressure can be consistently sampled independent of the effusion-cell. This condition is obtained with the inclusion of two fixed apertures (field and source) between the effusion cell and ion source and accurate alignment of the orifice [14,21–23]. The fixed apertures define an ionization volume independent of vapor source and the alignment of the orifice is monitored visually with a video camera mounted above the ion source that sights through the fixed apertures [14]. The temperature was measured with a pyrometer (Mikron M190V-TS) sighting a blackbody source (2.5 mm in diameter and 13.5 mm long) machined into the bottom of the effusion-cell and Mo-cell holder.

## 3. Results

$\text{Al}_2\text{O}_3$  condensed and clogged the effusion orifice over 8 h at  $T = 1550 \pm 3$  K and was observed visually and as a drop in the measured ion intensities of  $\text{Al}^+$  and  $\text{Al}_2\text{O}^+$  with time. In addition to growth on the outer edge of the effusion orifice,  $\text{Al}_2\text{O}_3$  “needles or whiskers” also grew from other surfaces in the furnace in a direct line from the effusion orifice. These areas are identified in the cross section of the furnace shown in figure 2. The extent of clogging after 8 h is shown in the SEM image of the outside of the orifice, shown in figure 3. The  $\text{Al}_2\text{O}_3$  crystals have grown out of the plane of the orifice ( $30\text{--}60^\circ$  to the normal) and range widely in thickness.

The temperature and instrument sensitivity were monitored during the experiment and the ion intensity of  $\text{Au}^+$  from the effusion cell containing pure  $\text{Au}(\text{l})$  is shown in figure 4. Over 8 h the furnace temperature slowly increased from  $T = (1547 \text{ to } 1552)$  K while the measure ion intensity,  $I_{\text{Au}}$ , remained consistent at  $5342 \pm 180$  cps. This indicates a small decrease in instrument sensitivity but this is not expected to affect any other results. The variation in the measured ion intensities of  $\text{Al}^+$ ,  $\text{Al}_2\text{O}^+$  and  $F$ , as the effusion orifice closed, are shown in figure 5. During an initial period,  $\sim 2$  h, the measured ion intensities of  $\text{Al}^+$  and  $\text{Al}_2\text{O}^+$  were constant. This is expected to be due to a “restricted collimation” condition imposed by the fixed apertures that define the source area,  $A_s$ , of the molecular beam that is smaller than the cross section of the effusion orifice,

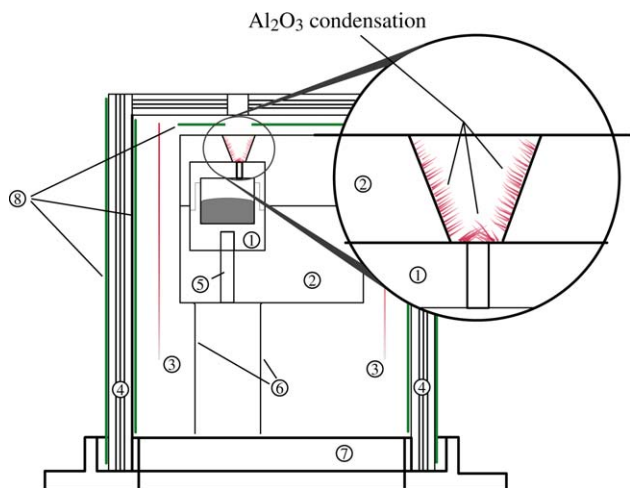


FIGURE 2. Schematic cross section of vapor source furnace with the insert showing detail of the areas where  $\text{Al}_2\text{O}_3$  condensation was observed. (1) Effusion-cell; (2) Mo envelope for 3 effusion-cells; (3) W-foil (25  $\mu\text{m}$  thick) heating element; (4) Ta heat shields; (5) blackbody source; (6) Ta light shield; (7) Mo heat shield support; and (8) additional Hf-foil ( $\sim 150$   $\mu\text{m}$  thick) “oxygen getter”.

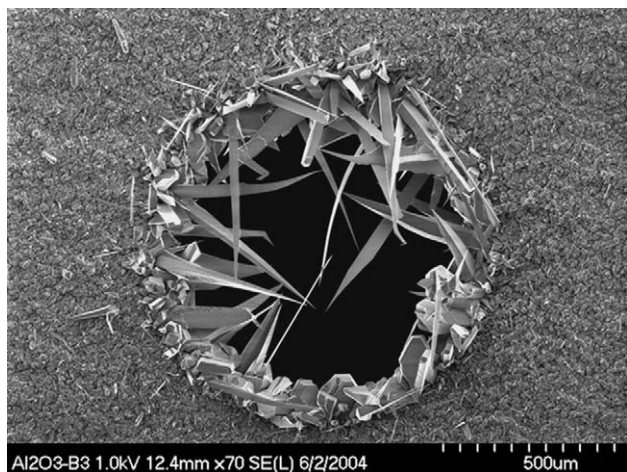


FIGURE 3. SEM image of  $\text{Al}_2\text{O}_3$  condensation and growth observed on the outer edge of the effusion orifice after 8 h at  $T = 1550 \pm 3$  K.

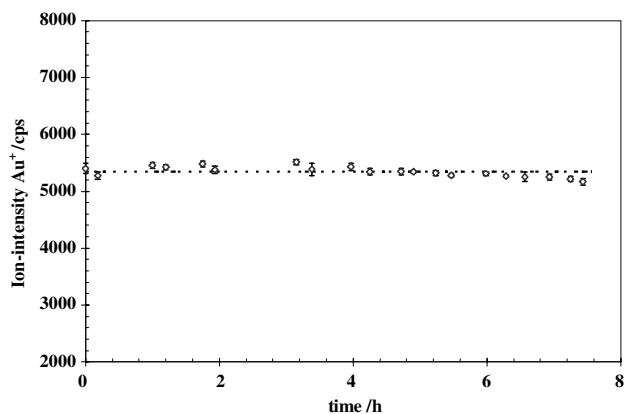


FIGURE 4. Plot of the measured ion intensity of  $\text{Au}^+$  versus time at  $T = 1550 \pm 3$  K.

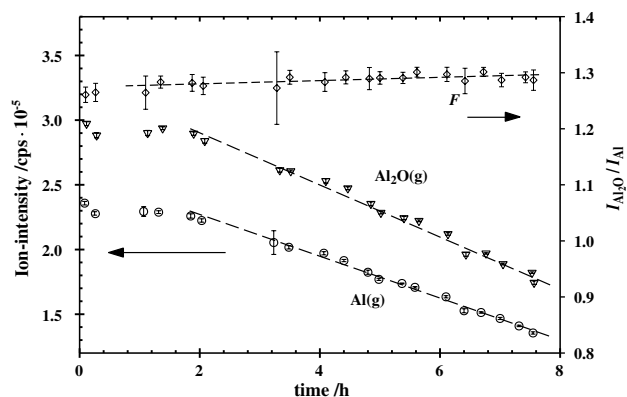


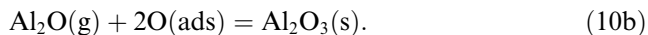
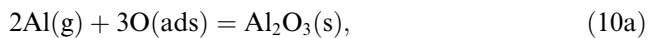
FIGURE 5. Plot of the measured ion intensities of  $\text{Al}^+$ ,  $\text{Al}_2\text{O}^+$  (left y-axis) and  $F = p(\text{Al}_2\text{O})/p(\text{Al})$  (right y-axis) versus time at  $T = 1550 \pm 3$  K as the orifice closed due to  $\text{Al}_2\text{O}_3$  condensation.

$A_o$  [22,23]. As a result the flux distribution of  $\text{Al}(\text{g})$  and  $\text{Al}_2\text{O}(\text{g})$  in the molecular beam remained relatively unchanged until the growth of  $\text{Al}_2\text{O}_3$  condensation encroaches into the source area,  $A_s$ . Following this initial period, the measured ion intensities of  $\text{Al}^+$  and  $\text{Al}_2\text{O}^+$  dropped about 41% over 6 h as the  $\text{Al}_2\text{O}_3$  crystals continued to grow.  $F$  remained consistent with only a small increase with time consistent with the measured temperature drift and the reaction enthalpies reported in table 1.

#### 4. Discussion

Observing that the measured ratio of  $p(\text{Al}_2\text{O})/p(\text{Al})$  remained consistent as the orifice closed provides direct evidence that hindered vaporization of  $\text{Al}(\text{g})$  from  $\text{Al}_2\text{O}_3(\text{s})$  inside the effusion cell is not the reason for the condensation of  $\text{Al}_2\text{O}_3$ . The condensation of  $\text{Al}_2\text{O}_3$  can be easily understood when it is recognized that inside the effusion cell  $\text{Al}(\text{g})$  and  $\text{Al}_2\text{O}(\text{g})$  are in equilibrium with  $\{\text{Al}(\text{l}) + \text{Al}_2\text{O}_3(\text{s})\}$  and this equilibrium also defines a partial pressure of  $\text{O}_2(\text{g})$  in the order of ( $10^{-42}$  to  $10^{-20}$ ) Pa or  $\text{O}(\text{g})$  ( $10^{-24}$  to  $10^{-12}$ ) Pa over the temperature range  $T = (1000$  to  $1600)$  K. The environment outside the effusion-cell in a furnace containing Ta can contain  $\text{O}_2(\text{g})$  pressures up to ( $10^{-29}$  to  $10^{-12}$ ) Pa [11]. This is many orders of magnitude higher than that in equilibrium with  $\{\text{Al}(\text{l}) + \text{Al}_2\text{O}_3(\text{s})\}$  which allows the  $\text{Al}_2\text{O}_3$  effusion-cell to remain stable. Therefore, as Al and  $\text{Al}_2\text{O}$  molecules leave the effusion cell they enter an environment with a greatly increased oxygen activity which results in a large driving force for  $\text{Al}_2\text{O}_3(\text{s})$  formation. At reduced pressures ( $\sim 10^{-4}$  Pa) a heterogeneous reaction between  $\text{Al}(\text{g})$ ,  $\text{Al}_2\text{O}(\text{g})$ , and absorbed oxygen ( $\text{O}_2$  or  $\text{O}$ ) on a surface is more probable than homogeneous precipitation of  $\text{Al}_2\text{O}_3(\text{s})$  in the vapor phase. The identity of the species providing oxygen is unknown but  $\text{O}_2(\text{g})$ ,  $\text{O}(\text{g})$ , and  $\text{H}_2\text{O}(\text{g})$  are all present the vacuum.

Therefore, it is proposed that  $\text{Al}_2\text{O}_3$  condensation occurs by heterogeneous growth by the reaction of impinging fluxes of  $\text{Al}(\text{g})$  or  $\text{Al}_2\text{O}(\text{g})$  molecules with oxygen containing species on a  $\text{Al}_2\text{O}_3$ -surface according to either:



It is unclear which reaction dominates the growth rate of  $\text{Al}_2\text{O}_3(\text{s})$ . This would be difficult to determine and is outside of the scope of this investigation. In general terms, the growth kinetics depend on: the flux of  $\text{Al}_2\text{O}(\text{g})$ ,  $\text{Al}(\text{g})$ , and oxygen containing species; their condensation coefficients; the adsorption process; and the crystallographic orientation of the  $\text{Al}_2\text{O}_3$  relative to the vapor flux [24]. According to this theory, as the temperature is increased the growth rate of condensed  $\text{Al}_2\text{O}_3$  will increase in proportion to  $p(\text{Al}_2\text{O})$  and  $p(\text{Al})$ , provided there is an adequate supply of oxygen. Therefore, the higher  $\text{Al}_2\text{O}_3$  growth rate observed in Motzfeldt's first study can probably be attributed to the higher temperatures ( $T = 1585$  K and  $T = 1623$  K as opposed to  $T = 1556$  K) rather than the different heating element materials (graphite and Mo).

Even though  $\text{Al}(\text{g})$  and  $\text{Al}_2\text{O}(\text{g})$  are reacting to form  $\text{Al}_2\text{O}_3(\text{s})$  this is not expected to change the measured  $p(\text{Al}_2\text{O})/p(\text{Al})$  ratio because only molecules that do not react to form  $\text{Al}_2\text{O}_3(\text{s})$  reach the ion-source. The molecular beam should therefore retain the equilibrium  $p(\text{Al}_2\text{O})/p(\text{Al})$  ratio defined by  $\text{Al}(\text{l}) + \text{Al}_2\text{O}_3(\text{s})$  inside the effusion-cell. Some vaporization will occur from the condensed  $\text{Al}_2\text{O}_3(\text{s})$  within the source area,  $A_s$ , of the molecular beam, however, the increased oxygen activity of the furnace environment mean  $\text{Al}_2\text{O}(\text{g})$  and  $\text{Al}(\text{g})$  no longer dominate. Therefore, the contribution of  $\text{Al}_2\text{O}(\text{g})$  and  $\text{Al}(\text{g})$  vaporizing from the condensed  $\text{Al}_2\text{O}_3(\text{s})$  to the molecular beam should be insignificant compared to that coming from within the effusion cell, until the point when the orifice is almost completely closed. Therefore, clogging of the orifice by  $\text{Al}_2\text{O}_3$  condensation can be thought of solely as changing the effective orifice-area and the associated change in the distribution of effusing molecules. As orifice clogging is more pronounced at high temperatures, pressure measurements made at higher temperatures are more effected, reducing the measured enthalpies of vaporization of both  $\text{Al}(\text{g})$  and  $\text{Al}_2\text{O}(\text{g})$ , as seen in table 1. Improving thermodynamic measurements in the Al–O system requires that the effect of  $\text{Al}_2\text{O}_3$  condensation is reduced to a minimum.

#### 4.1. Suggestions for improved thermodynamic measurements

According to this theory, the condensation of  $\text{Al}_2\text{O}_3(\text{s})$  must occur at all temperatures but it only occurs at an observable rate when  $p(\text{Al})$  and  $p(\text{Al}_2\text{O})$  are

high enough to provide a significant molecular flux to the  $\text{Al}_2\text{O}_3$ -surface for a given  $p(\text{O}_2)$ . Therefore, more accurate thermodynamic data in the Al–O system can be obtained by: (1) limiting measurements to temperatures below about 1450 K with the highest temperature measurement taken first or (2) reducing the  $p(\text{O}_2)$  inside the furnace to levels that approach those in equilibrium with  $\{\text{Al}(\text{l}) + \text{Al}_2\text{O}_3(\text{s})\}$ . The first option may not initially appear satisfactory, however, the upper pressure-limit of the Knudsen-effusion technique ( $\sim 1$  Pa), imposed by molecular flow conditions, already limits the temperature to about  $T = 1600$  K. Reducing  $p(\text{O}_2)$  to these levels requires the introduction of “oxygen-getters” (in the form of Ti, Zr, or Hf sheets) inside the multiple effusion cell furnace and the vacuum chamber. These have been added to the furnace as shown in figure 2 but additional heated sheets are probably required outside the furnace, particularly around the field aperture and also inside the ion source chamber. Obviously, there is a limit to reducing  $p(\text{O}_2)$  as the  $\text{Al}_2\text{O}_3$  effusion-cell must remain stable. It is also important to notice that this behavior is likely to occur in other metal-oxygen systems that contain very stable oxides, for example Y–O, Zr–O, Ti–O.

## 5. Conclusions

In an effort to better determine the thermodynamic properties of vapor species in the Al–O system the problem of  $\text{Al}_2\text{O}_3$  condensation and orifice clogging was reconsidered. Motzfeldt's theory for  $\text{Al}_2\text{O}_3$  condensation was reviewed and serious questions were raised about its validity. This theory was based on the apparent increase in  $p(\text{Al}_2\text{O})/p(\text{Al})$  with effusion orifice area and this was attributed to “hindered” vaporization of  $\text{Al}(\text{g})$  from  $\text{Al}_2\text{O}_3(\text{s})$ . This study tested this assumption by monitoring  $p(\text{Al}_2\text{O})/p(\text{Al})$  over 8 h at  $T = 1550 \pm 3$  K while the effusion orifice clogged due to the growth of  $\text{Al}_2\text{O}_3$  crystals. A consistent  $p(\text{Al}_2\text{O})/p(\text{Al})$  ratio was observed during this period while the measured partial pressures of  $\text{Al}_2\text{O}(\text{g})$  and  $\text{Al}(\text{g})$  both dropped about 41%. This disagrees with the previous explanation for  $\text{Al}_2\text{O}_3$  condensation. A much simpler explanation was proposed based on the large difference in  $p(\text{O}_2)$  between the inside of the effusion cell (defined by the  $\{\text{Al}(\text{l}) + \text{Al}_2\text{O}_3(\text{s})\}$  equilibrium) and the furnace environment. As the Al and  $\text{Al}_2\text{O}$  molecules leave the effusion-cell they enter an environment with a greatly increased  $p(\text{O}_2)$  and  $\text{Al}_2\text{O}_3$  condensation occurs by heterogeneous growth by the reaction of impinging  $\text{Al}(\text{g})$  or  $\text{Al}_2\text{O}(\text{g})$  molecules with absorbed O on a  $\text{Al}_2\text{O}_3$ -surface. According to this theory  $\text{Al}_2\text{O}_3$  condensation occurs at all temperatures while studying  $\{\text{Al}(\text{l}) + \text{Al}_2\text{O}_3(\text{s})\}$  but it only occurs at an observable rate at temperatures above  $T = 1500$  K when the fluxes of  $\text{Al}(\text{g})$  and  $\text{Al}_2\text{O}(\text{g})$  are high. To obtain more accurate thermodynamic data in the Al–O system it was

proposed to either: (1) limit measurements to below 1450K with the highest temperature measurement taken first or (2) reduce the  $p(\text{O}_2)$  inside the furnace to levels that approach the dissociation pressure in equilibrium with  $\{\text{Al}(\text{l}) + \text{Al}_2\text{O}_3(\text{s})\}$ . A combination of both is currently being tried.

### Acknowledgements

The help of Christian Chatillon and Nathan Jacobson in preparing this manuscript and providing insightful discussion is gratefully acknowledged. The funding for this work came from NASA Glenn Research Centre's Low Emission Alternative Power Project.

### References

- [1] L. Brewer, A. Searcy, J. Am. Chem. Soc. 73 (1951) 5308–5314.
- [2] R. Porter, P. Schissel, M. Inghram, J. Chem. Phys. 23 (1955) 339–342.
- [3] O. Herstad, K. Motzfeldt, Rev. Hautes Temper. et Refract. 3 (1966) 291–300.
- [4] D.B. Rao, K. Motzfeldt, Acta Chem. Scand. 24 (1970) 2796–2802.
- [5] J. Drowart, G. DeMaria, R.P. Burns, M.G. Inghram, J. Chem. Phys. 32 (1960) 1366–1372.
- [6] G. De Maria, J. Drowart, M.G. Inghram, J. Chem. Phys. 30 (1959) 318–319.
- [7] E. Copland, Z. Metallkd. (2005), accepted.
- [8] T. Markus, K. Hilpert, in: E. Opila, J. Fergus, T. Maruyama, J. Mizusaki, T. Narita, D. Shifler, E. Wuchina (Eds.), High Temperature Corrosion and Materials Chemistry, V, The Electrochemical Society, Hawaii, 2004.
- [9] M. Heyrman, C. Chatillon, J. Phys. Chem. Solids 66 (2005) 494–497.
- [10] E. Copland, in: E. Opila, J. Fergus, T. Maruyama, J. Mizusaki, T. Narita, D. Shifler, E. Wuchina (Eds.), High Temperature Corrosion and Materials Chemistry, V, The Electrochemical Society, Hawaii, 2004.
- [11] L.V. Gurvich, I.V. Veyts, C.B. Alcock, Thermodynamic Properties of Individual Substances, Begell House, 1996, English Version.
- [12] M. Chase, NIST-JANAF Thermochemical Tables, American Chemical Society, 1998.
- [13] CODATA Key Values for Thermodynamics, Hemisphere Publishing Corp., Washington, 1988.
- [14] E. Copland, N. Jacobson, NASA Report, 2005, unpublished results.
- [15] H. Wriedt, Bull. Alloy Phase Diagrams 6 (6) (1985) 548–553, 567–568.
- [16] M. Rother, H. Holleck, J. Chim. Phys. Phys. Chim. Biol. 90 (1993) 333.
- [17] S. Lakiza, L. Lapato, J. Am. Ceram. Soc. 80 (1997) 893–902.
- [18] O. Fabrichnaya, F. Aldinger, Z. Metallkd. 95 (2004) 27–39.
- [19] G. Rosenblatt, in: N. Hannay (Ed.), Treatise on Solid State Chemistry, Surfaces I, vol. 6A, Plenum Press, New York, 1976, pp. 165–240 (Chapter 3).
- [20] M. Inghram, J. Drowart, Mass Spectrometry Applied to High Temperature Chemistry, High Temperature Technology, Stanford Research Institute, California, 1959, pp. 338–378.
- [21] C. Chatillon, C. Senillou, M. Allibert, A. Pattoret, Rev. Sci. Instrum. 47 (1976) 334–340.
- [22] P. Morland, C. Chatillon, P. Rocabois, High Temp. Mater. Sci. 37 (1997) 167–187.
- [23] C. Chatillon, L. Malheiros, P. Rocabois, M. Jeymond, High Temp. High Press. 34 (2002) 213–233.
- [24] R. Voorhoeve, in: N. Hannay (Ed.), Treatise on Solid State Chemistry, Surfaces I, vol. 6A, Plenum Press, New York, 1976, pp. 241–342 (Chapter 4).

JCT 05-97